A Numerical Study of Hydrodynamic Processes and Flood Mitigation in a Large River-lake System

Hongwu Tang[1] · Hao Cao[2] · Saiyu Yuan[1] · Yang Xiao[1] · Chenyu Jiang[2] · Carlo Gualtieri[3]

Abstract

Floods out of all other water problems cause very large damages in China. Previous flood management plans mainly focused on a single river by controlling its water level and conveyance capacity, while research on mitigation solutions to flooding issues in river-lake systems is scarce. This study considers the Huai River - Lake Hongze system, which is one of the largest river-lake systems in China. Very large damages associated with small floods are frequently observed in this river-lake system, although a series of flood management measures have been implemented in the Huai River Basin since the middle of the last century. An unstructured-grid finite-volume numerical model was applied to simulate hydrodynamic processes in this system, which is characterized by discrepant spatial scales between these two types of water bodies. It is found that the lake affects the upstream river flooding, but lowering the lake level would have limited effects that would be rapidly impaired by the sharp meander bend connecting the river and the lake. The artificial cutoff of this intensively-embanked bend has great potential in reducing the river stage and flood damages, as the construction of a diversion channel would shorten the flow path and increase the hydraulic gradient. This study extends the current knowledge about the hydrodynamics of river-lake systems and is beneficial to flood mitigation strategies for similar systems.

✉ Saiyu Yuan
  yuansaiyu@hhu.edu.cn

[1] State Key Laboratory of Hydrology-Water Resources and Hydraulic Engineering, Hohai University, Nanjing 210098, China

[2] College of Water Conservancy and Hydropower Engineering, Hohai University, Nanjing 210098, China

[3] Department of Civil, Architectural and Environmental Engineering (DICEA), University of Naples Federico II, Naples 80125, Italy

1 Introduction

Floods, more than other water problems, cause the most damage and have taken a severe toll on reduction in crop yield, heavy casualties, and huge economic losses in China (Zhao et al. 2014). According to the Bulletin of Flood and Drought Disasters in China (Ministry of Water Resources of the People's Republic of China 2019), annual direct monetary loss caused by floods from 1990 to 2018 was 150.90 billion RMB on average (about 21.35 billion US dollars). Conventional measures for flood management include (1) structural types of reservoirs on the upper reach, retention areas, dams and sluices, flood bypasses, dykes, and dredging (Hudson et al. 2008; Zhang et al. 2010; Zhang and Song 2014; Wan et al. 2018); and (2) non-structural types of flood forecasting by hydro-meteorological modeling or machine learning, and flood monitoring by remote sensing (Zheng et al. 2008; Lin et al. 2010; Liu et al. 2017). These measures are mainly control-oriented and emphasize the water level and conveyance capacity of a single river. However, studies on flood mitigation in a river-lake system are scarce. In the Huai River Basin in East China, a series of flood management plans have been implemented since the middle of the last century (For instance, 38 large reservoirs have been built on the upper reach), but large damages caused by small but prolonged floods are still frequently observed (Qian and Wang 2017). Those frequent flooding is closely related to the hydrodynamics of the river-lake system.

Complex interactions between large lakes and rivers are usually the causes of flooding, water impurity and other water problems (Paturi et al. 2012; Wu et al. 2012). Two different conditions were considered in previous studies. The first one is that the river plays the role of mainstream and the lake is treated as a tributary of the river. The complex hydrodynamic processes at the confluence are controlled by the confluence geometry, the discharge ratio between the confluent flows, the level of concordance between channel beds at the confluence entrance, the water level and any eventual difference in water density between the tributaries (Ianniruberto et al. 2018; Gualtieri et al. 2019). For instance, the two largest freshwater lakes in China, i.e. Lake Poyang and Lake Dongting, are tributaries of the Yangtze River. The operations of Three Gorges Dam project in the upstream Yangtze River, caused large variation of discharge processes and are responsible for the advanced and lengthened dry seasons of Lake Poyang (Dai et al. 2017; Zhang et al. 2018; Wang et al. 2015). In the second type the large river is regarded as the largest or one of the largest tributaries feeding the lake. River flooding carries sediment, pollutants and other materials downstream into the lake. The transport processes from the river to the lake have been studied in some systems, e.g. the Lake Winnipeg - Red River system (Rao and Zhao 2010), the Lake Michigan - Grand River Michigan system (Nekouee et al. 2015), the Lake Erie - Grand River Ontario system (He et al. 2006), and the Lake Kinneret - Jordan River system (Ben-Dan et al. 2001). These studies mainly investigated the effects of the river on the lake, while only a few references attempted to illustrate the reverse effects of the lake on the river, such as the influence of lake seiches on contaminant transport in the Lake Superior - St. Louis River system (Sorensen et al. 2004) and the hydrodynamic process in the St. Clair River - Lake St. Clair - Detroit River system (Shore 2009). In the present study, the authors attempt to consider the Huai River - Lake Hongze system as a hotspot where the role played by the lake on the prolonged flooding in the upstream large river needs to be identified.

The primary task here is to investigate the hydrodynamic interactions between the lake and the river. Given the large variations of spatial scales in river-lake systems, the FVCOM model (Finite-Volume Community Ocean Model), a 3-D unstructured-grid model (Chen et al. 2003,

2006), was applied. This model has been recognized as reliable for characterizing the hydrodynamic behavior in river-lake systems (Shore 2009; Bai et al. 2013; Huang and Li 2017).

This paper is divided into five main sections. Following the Introduction, the details about the physical setting of the study area and proposed flood management plans were described. Secondly, the set-up of the numerical simulations, especially the compensation method for water budget in an intensively-regulated system, were presented. Thirdly, the hydrodynamic characteristics of the study area were analyzed in the lake and the transition reaches, respectively. Then, the mechanism of prolonged flooding was discussed by numerical experiments and alternative flood mitigation solutions were accordingly evaluated. Finally, conclusive remarks about the hydrodynamic interactions between Lake Hongze and the Huai River were presented.

2 Physical Setting

2.1 Study Area

The Huai River Basin (111°55′–121°20′E, 30°55′–36°20′N) is located in East China (Fig. 1), which has a catchment area of 270 thousand km². Its middle reach has a length of 490 km, while the difference of the ground elevation is only 16 m, i.e. the slope is about 0.33‰ (Yu et al. 2014). Lake Hongze, the fourth largest freshwater lake in China, is located on the downstream reach of the Huai River. Corresponding to lake level of 13.5 m, its storage volume is 4.23 billion m³ and surface area is 1542 km².

The Huai River is located at about the midway between the Yellow River and the Yangtze River. It heads on the Tongbai Mountains of Henan Province and flows east. Before 1194, the Paleo-Huai River directly discharged into the Yellow Sea, but from XII to XIX century, the hyper-concentrated flow from the Paleo-Yellow River filled the passage of the Paleo-Huai River entering the sea, and Lake Hongze was formed (Wang and Chen 1999). Nowadays, the elevation of Lake Hongze basin is higher than that of the thalweg of the upper reach (Fig. 2).

The Bengbu Sluice, the lowest sluice on the Huai River, is selected as the upstream boundary of the study area. The outlets of Lake Hongze act as downstream boundaries. The length of the Huai River in the study area (from the Bengbu Sluice to Laozishan) is about 182 km (Fig. 3). The reach is composed of quasi-straights, bends and anabranches. There is a main tributary in this reach, i.e. the Chi River with a catchment area of 4248 km². Lake Hongze has mainly six inflows and four outflows (Fig. 1).

2.2 Proposed Flood Management Plans

The flooding in the middle Huai River Basin is frequent and severe. When a storm flood occurs, the floodwater from southern hilly regions first reaches the Huai River. Due to the poor drainage condition of the Huai River, the river stage rises quickly, but declines slowly. As a consequence of the backwater effect of the Huai River, prolonged flooding is also observed in the northern tributaries. Great efforts have been made for the flood control in this region (Qian and Wang 2017), but with limited results. In the 2007 basin-wide flood disaster more than 800,000 persons lost their houses and direct economic losses were estimated as 15.52 billion RMB (about 2.21 billion US dollars).
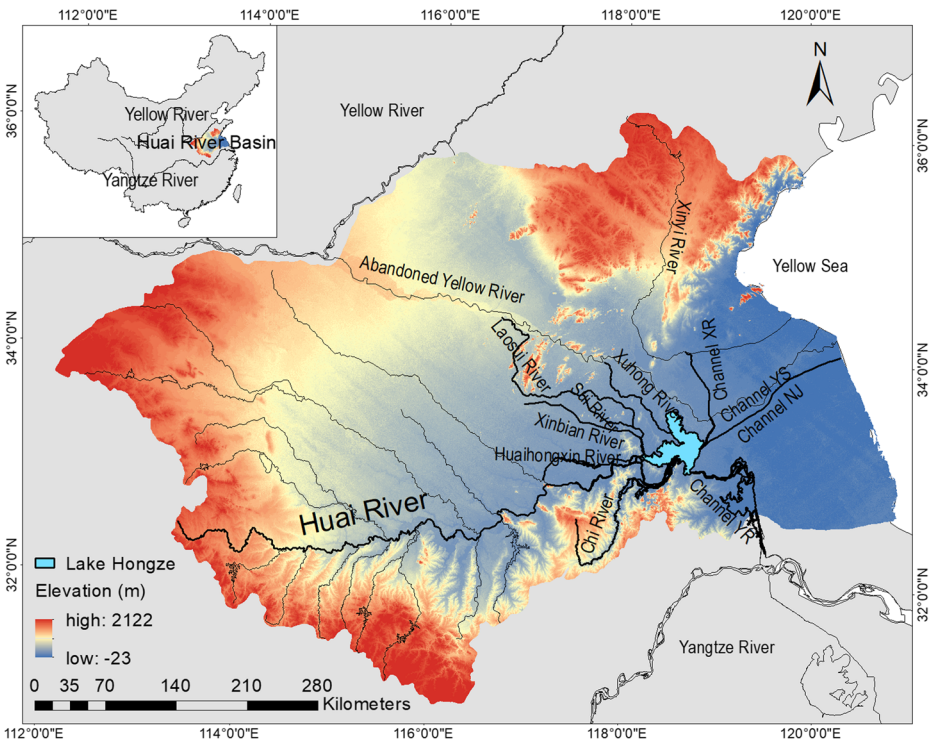
Fig. 1 Sketch map of the Huai River Basin with topographic contours (Note, the elevation is above the national benchmark named after the Abandoned Yellow River). Besides the Huai River, the other five main inflows include the Huaihongxin River, the Xinbian River, the Sui River, the Laosui River, and the Xuhong River. Four main outflows include the Channel into the Yangtze River (the Channel YR), the Main Irrigation Channel in North Jiangsu (the Channel NJ), the Channel into the Yellow Sea (the Channel YS), and the Channel into the Xinyi River (the Channel XR)

Common measures, such as the reclamation of land from the river and the establishment and proper usage of retention areas, can hardly be implemented due to safety reasons for riverside residents (Han and Suryadi 2004). Considering all these limiting factors, three different management plans (Case 1: lowering the lake level; Case 2: dredging the channel of negative slope and the lake basin, shown in Fig. 4; Case 3: diverting the river flood at upstream of the negative-slope reach, shown in Fig. 5) were proposed and compared in this study. The results are useful to (1) identify the role that Lake Hongze is playing in prolonged river flooding and (2) provide a feasible mitigation solution.

3 Hydrodynamic Simulation of the River-lake System

3.1 FVCOM Model Set-ups

The study domain consists of both riverine and lacustrine reaches, where different spatial resolutions are required. The unstructured triangular grid adopted by FVCOM can meet the requirement of geometric flexibility. In the river, near the thalweg a grid resolution of 50 m was used and decreased transversely. In the lake, a grid resolution of 500 m was generally
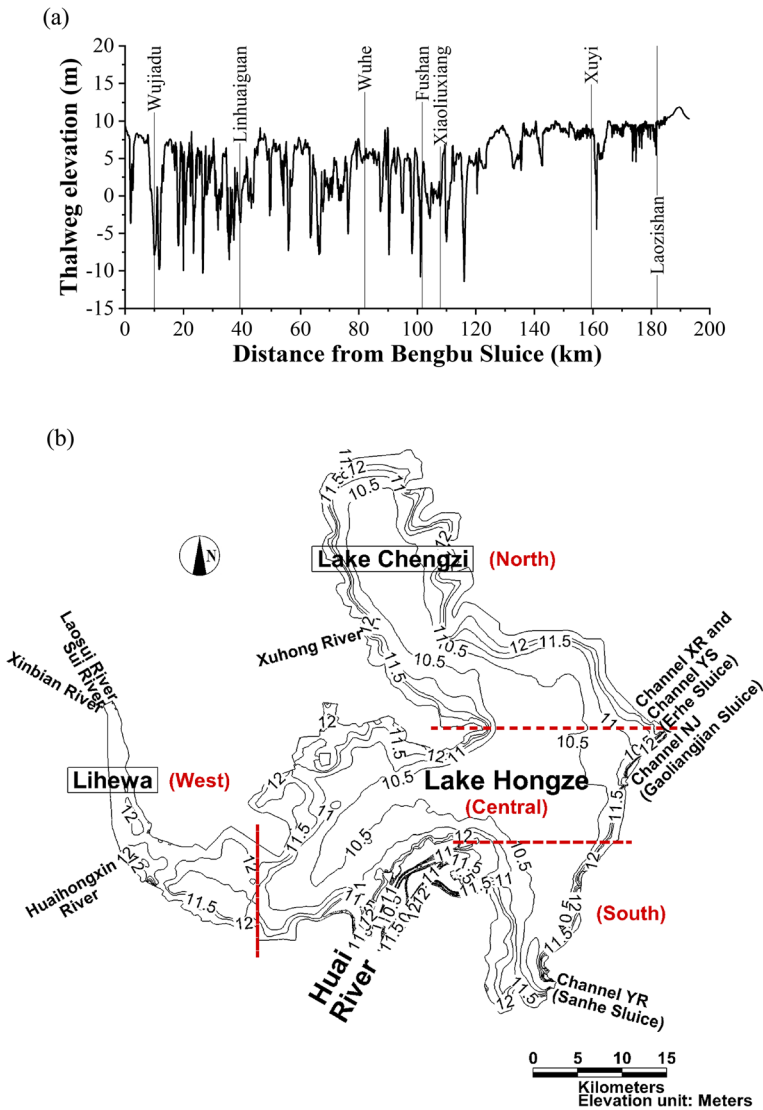
Fig. 2 Topographic map (Note, bathymetric surveys of Lake Hongze and the Huai River were carried out in the year of 2010 and 2013, respectively): (**a**) the Huai River; and (**b**) Lake Hongze. Moreover, the Lake Hongze is divided into four regions, i.e. Central, South, West (Lihewa) and North (Lake Chengzi) parts

used, but refined to 100 m near the lake inlets/outlets. The number of nodes and cells were 61,491 and 115,582, respectively (Fig. 3). Five vertical sigma layers were applied. For the computation of horizontal velocity components, a 0.1-to-0.4-second external time step was applied. The internal time step for the computation of vertical component was ten times larger than the external value. FVCOM ran on Linux system using the parallel computation mode. Modelling a year-round case with a 4×16-thread computer cluster needed five days for completion.
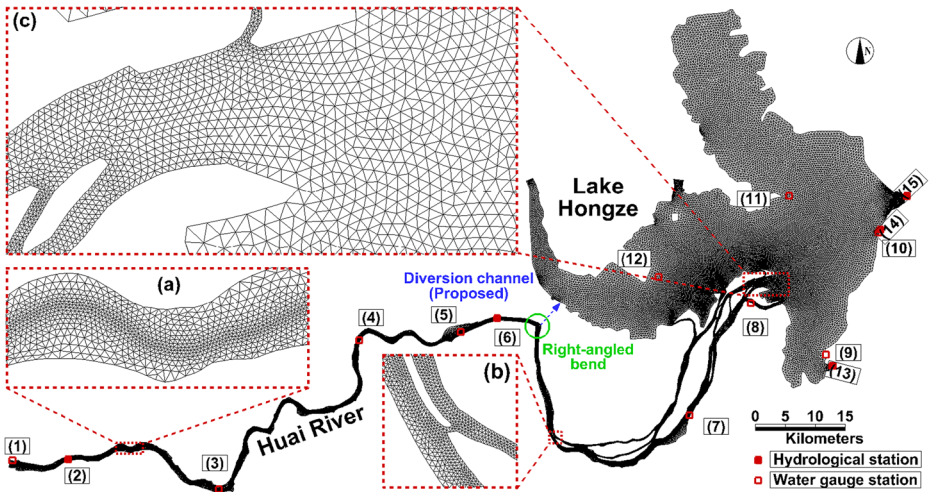
Fig. 3 Unstructured grid applied in the model, and three enlarged views of the grid at (**a**) riverine, (**b**) anabranching, and (**c**) lacustrine reaches. The positions of five hydrological stations (No. 2, 6, 13–15; red solid squares) and ten water gauge stations (No. 1, 3–5, 7–12; red hollow squares) are marked, as well as the right-angled bend (green solid circle) and the proposed diversion channel (blue dashed arrow). Fifteen stations include: (1) Bengbu Sluice; (2) Wujiadu; (3) Linhuaiguan; (4) Wuhe; (5) Fushan; (6) Xiaoliuxiang; (7) Xuyi; (8) Laozishan; (9) Jiangba; (10) Gaoliangjian; (11) Shangzui; (12) Linhuaitou; (13) Sanhe Sluice; (14) Gaoliangjian Sluice; (15) Erhe Sluice

FVCOM solves the conservation of momentum and mass equations (Chen et al. 2003):

$$
\begin{cases}
\frac{\partial u}{\partial t} + u\frac{\partial u}{\partial x} + v\frac{\partial u}{\partial y} + w\frac{\partial u}{\partial z} - fv = -\frac{1}{\rho_w}\frac{\partial P}{\partial x} + \frac{\partial}{\partial z}\left(K_m \frac{\partial u}{\partial z}\right) + F_u \\
\frac{\partial v}{\partial t} + u\frac{\partial v}{\partial x} + v\frac{\partial v}{\partial y} + w\frac{\partial v}{\partial z} - fu = -\frac{1}{\rho_w}\frac{\partial P}{\partial y} + \frac{\partial}{\partial z}\left(K_m \frac{\partial v}{\partial z}\right) + F_v \\
\frac{\partial P}{\partial z} = -\rho_w g
\end{cases}
\tag{1}
$$

$$
\frac{\partial u}{\partial x} + \frac{\partial v}{\partial y} + \frac{\partial w}{\partial z} = 0
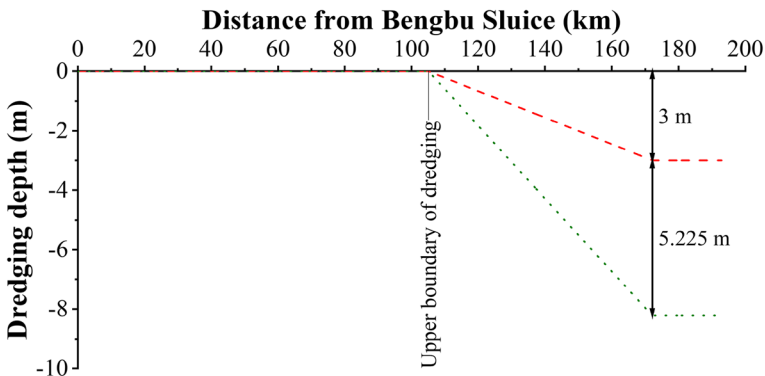\tag{2}
$$

Fig. 4 Dredging depths of two plans (green dotted and red dashed lines are Cases 2A and 2B, respectively). Note, the dredging depth of the lake basin is set as constant, i.e. the maximum dredging depth in the river reach
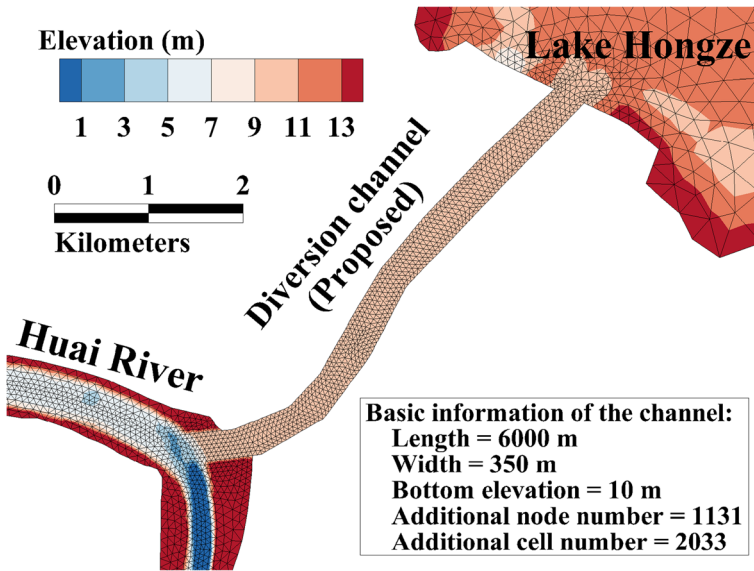
Fig. 5 Grid applied for the proposed diversion channel (Case 3)

where x, y and z are East, North and vertical axes in the Cartesian coordinate system; u, v and w are x, y and z velocity components; t is time; ρ_w is water density; P is pressure; f is Coriolis parameter; g is gravitational acceleration; K_m is vertical eddy viscosity coefficient; F_u and F_v are horizontal momentum diffusion terms.

3-D governing equations are applicable to simulate the river and lake with a dominant process in XZ plane and XY plane, respectively, in the same model. The horizontal eddy diffusion coefficient for momentum is calculated using the Smagorinsky (1963) eddy parameterization method adopting a constant coefficient of 0.2. The vertical eddy viscosity coefficient K_m is parameterized using Mellor and Yamada (1982) level 2.5 (MY-2.5) turbulent closure model as modified by Galperin et al. (1988). The wet/dry point treatment method is used corresponding to a minimum water depth of 0.05 m.

The surface and bottom boundary conditions for u, v, and w (Chen et al. 2003) are:

$$K_m\left(\frac{\partial u}{\partial z}, \frac{\partial v}{\partial z}\right) = \frac{1}{\rho_w}\left(\tau_{sx}, \tau_{sy}\right), w = \frac{\partial \zeta}{\partial t} + u\frac{\partial \zeta}{\partial x} + v\frac{\partial \zeta}{\partial y} + \frac{E-P}{\rho}, \text{ at } z = \zeta(x,y,t) \qquad (3)$$

$$K_m\left(\frac{\partial u}{\partial z}, \frac{\partial v}{\partial z}\right) = \frac{1}{\rho_w}\left(\tau_{bx}, \tau_{by}\right), w = -u\frac{\partial H}{\partial x} - v\frac{\partial H}{\partial y}, \text{ at } z = -H(x,y) \qquad (4)$$

where $\left(\tau_{sx}, \tau_{sy}\right) = C_{sd}\rho_a U_{10}\left(U_{10x}, U_{10y}\right)$ and $\left(\tau_{bx}, \tau_{by}\right) = C_{bd}\rho_w\sqrt{u^2 + v^2}(u, v)$ are x and y components of surface wind and bottom stresses, and C_{sd} and C_{bd} are corresponding drag coefficients; U_{10} is 10-m height wind speed, and U_{10x} and U_{10y} are x and y components; ρ_a is air density; ζ is height of free surface and H is bottom depth (relative to $z = 0$); P and E are precipitation and evaporation.

The surface drag coefficient C_{sd} was set equal to 0.0012 considering both shallow water of Lake Hongze and low wind speed of no larger than 11 m/s. To ensure stable computation, the bottom drag coefficient C_{bd} was assumed to be constant, but for channel floodplain, C_{bd} = 0.01, else, C_{bd} = 0.0025, as suggested by Ben (2010).
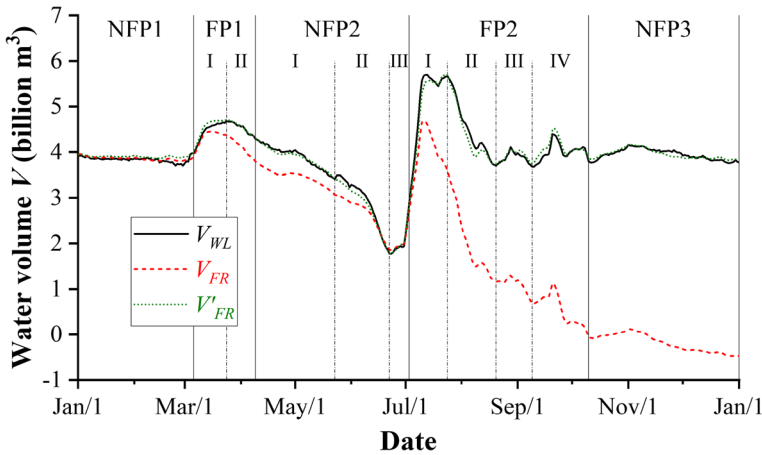
Fig. 6 Temporal distributions of water volume based on measured water level data V_{WL} (solid lines), measured discharge data V_{FR} (dashed lines) and compensated data V'_{FR} (dotted lines) in the study area (Note, precipitation and evaporation are also included in the calculation of V_{FR} and V'_{FR})

The 2007 basin-wide flood event with a return period of 20 years was chosen for this study. The temporal distributions of water volume in the study area based on measured water level data (V_{WL}) and measured discharge data (V_{FR}) are presented in Fig. 6, and an overall shortage of inflows was observed. The Channel YR is used when large flows occur in the upstream Huai River Basin, hence the usage or not of the channel can reflect the flood and non-flood periods. In accordance to this classification, the modeled period of one year was divided into segments like: (1) non-flood periods: NFP1 from January 1 to March 6, NFP2 from April 10 to July 3, and NFP3 from October 11 to December 31, respectively; (2) a spring flood FP1 from March 7 to April 9; (3) a summer flood FP2 from July 4 to October 10. To evaluate and compensate the un-/mis-measured terms, the water balance for a water body for specific periods (Sokolov and Chapman 1974) is computed by:

$$P + Q_I - E - Q_O - \Delta V - \eta = 0 \tag{5}$$

Table 1 Water balance computations throughout the modeled year

Period	P (mm)	Q_I	E	Q_O	ΔV	η	$\bar{\eta}$	ε (%)
NFP1	72.2	968.4	83.4	978.8	31.6	-53.1	-0.8	-2.5
FP1-I	25.2	1222.6	33.6	920.9	448.2	-155.0	-8.6	-7.0
FP1-II	16.3	614.9	46.3	947.0	-246.2	-115.9	-7.2	-7.1
NFP2-I	40.4	660.1	159.4	994.5	-555.6	102.1	2.3	5.5
NFP2-II	50.8	163.4	118.2	844.7	-1035.4	286.6	9.6	24.4
NFP2-III	215.7	539.8	27.6	208.9	694.4	-175.4	-15.9	-17.7
FP2-I	456.6	10450.7	40.1	10342.1	1767.7	-1242.6	-59.2	-5.8
FP2-II	128.0	9365.1	97.0	10944.1	-1243.7	-304.3	-11.3	-1.5
FP2-III	75.6	3916.0	57.5	4229.5	-12.6	-282.7	-14.1	-3.4
FP2-IV	200.2	2233.1	85.5	2813.2	75.8	-541.2	-17.5	-10.2
NFP3	76.2	1577.1	122.7	1802.5	-18.9	-252.9	-3.0	-7.1
Summation	1357.0	31711.3	871.2	35026.2	-94.7	-2734.3	-7.5	-4.0

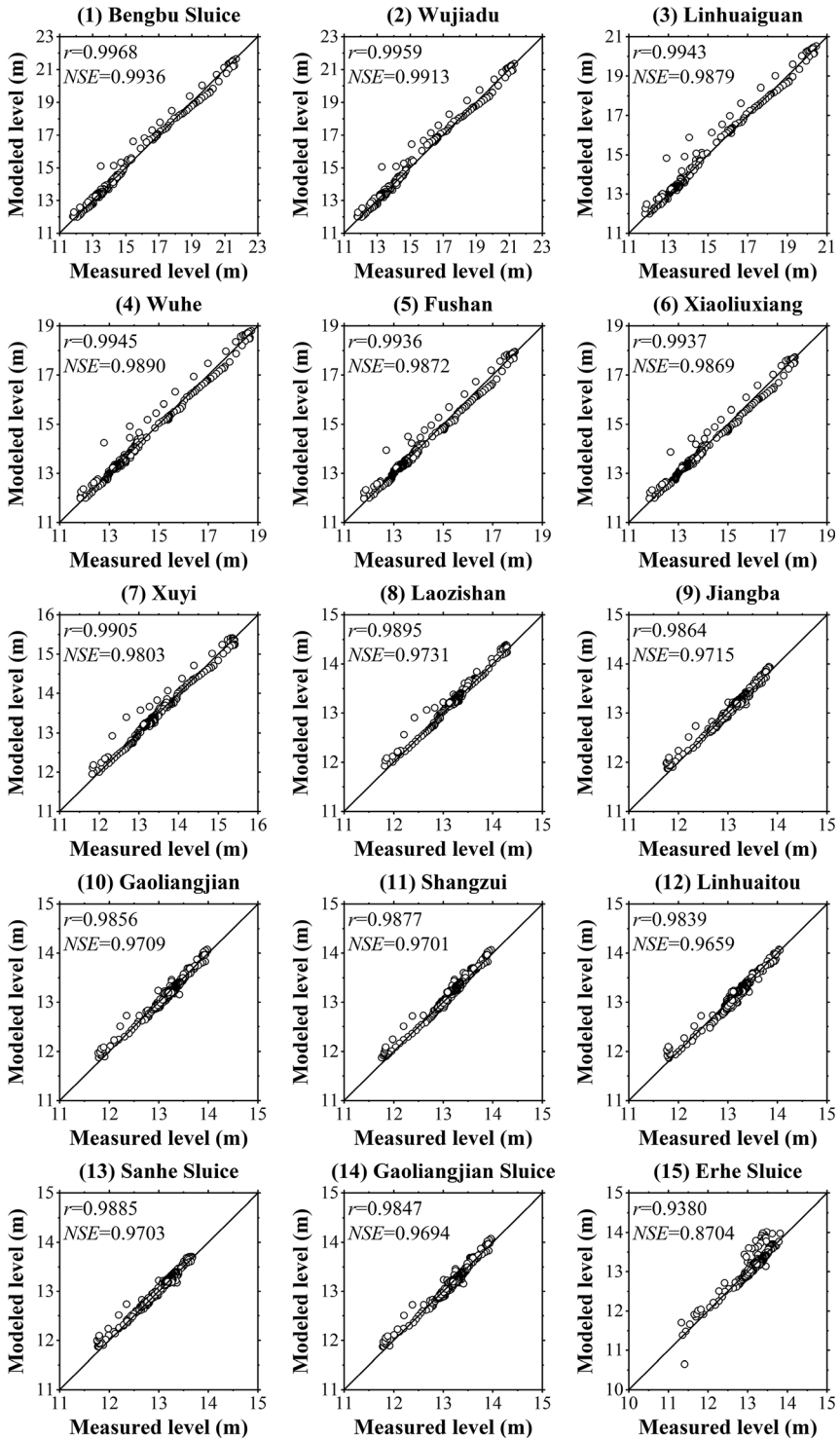* Area of the water body is assumed to be 1584 km² under the water level of 13.2 m

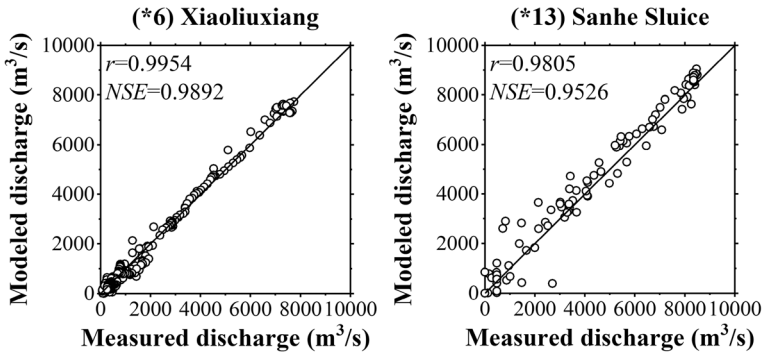**Fig. 7** Measured and modeled water levels at all fifteen stations

Fig. 8 Measured and modeled flow rates at two key stations

where Q_I and Q_O are river inflow/outflow discharges from the water body; ΔV is the total storage in the body; η is the discrepancy term. Note, the components of the above equation are expressed as a mean depth of water over the water body (mm). Moreover, to trace extreme conditions as flood peaks, ascending and descending segments are separated in the periods with large fluctuation of ΔV, i.e. FP1, NFP2 and FP2 (Fig. 6). The results throughout the year are listed in Table 1. Only in NFP2-I and NFP2-II (pre-release period), the time-averaged discrepancy $\bar{\eta}$ over a specified period is positive, which shows a shortfall of outflows from the water body. To compensate for the water budget, the compensation factor ε is introduced, defined as $\eta/(P+Q_I+E+Q_O)$. Components will be updated to $(1-\varepsilon)P$, $(1-\varepsilon)Q_I$, $(1+\varepsilon)E$ and $(1+\varepsilon)Q_O$, respectively. The temporal distribution of water volume based on compensated components (V'_{FR}) is plotted in Fig. 6.

The discharges of rivers/channels were included from the solid boundary, an exception being the main outflow during FP2 (i.e. Channel YR) where the open boundary condition was adopted. This setup is beneficial to the computational stability. The model was initialized in five days from December 27 to 31, 2006.
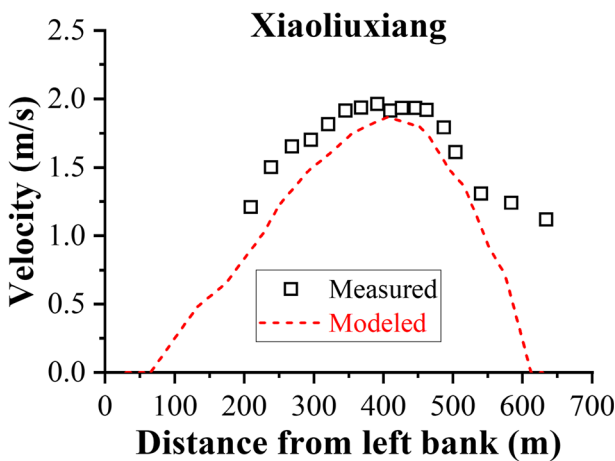

Fig. 9 Measured and modeled transverse distribution of depth-averaged velocity at Xiaoliuxiang (Note, the measured data is on July 15, 2003, correspondingly the discharge at Xiaoliuxiang $Q_{XLX} = 7780$ m^3/s and the water level $Z_{XLX} = 17.99$ m; the numerical result is on July 20, 2007, corresponding $Q_{XLX} = 7740$ m^3/s and $Z_{XLX} = 17.73$ m)

3.2 Model Evaluation

Five hydrological stations and ten water gauge stations are distributed in the whole study area (Fig. 3), and the field measurements and numerical results for the water levels are compared in Fig. 7. Among them, discharge data from two key stations (No. 6 and 13) were used to be compared with the modeled results (Fig. 8). The correlation index, including correlation coefficient (r) and coefficient of efficiency (NSE; Nash and Sutcliffe 1970), were included in the figures. Measured data by Ben (2010) and numerical results for the transverse distribution of velocity at Xiaoliuxiang corresponding to similar conditions of discharge and water level are compared in Fig. 9.

$$r = \frac{\sum\limits_{n=1}^{N} \left(Z_{measured}^n - \overline{Z}_{measured} \right) \left(Z_{modeled}^n - \overline{Z}_{modeled} \right)}{\sqrt{\sum\limits_{n=1}^{N} \left(Z_{measured}^n - \overline{Z}_{measured} \right)^2 \sum\limits_{n=1}^{N} \left(Z_{modeled}^n - \overline{Z}_{modeled} \right)^2}} \tag{6}$$

$$NSE = 1 - \frac{\sum\limits_{n=1}^{N} \left(Z_{measured}^n - Z_{modeled}^n \right)^2}{\sum\limits_{n=1}^{N} \left(Z_{measured}^n - \overline{Z}_{measured} \right)^2} \tag{7}$$

where N is the number of data points; $Z_{modeled}^n$ is the value of the nth modeled results; $Z_{measured}^n$ is the value of the nth measured data; $\overline{Z}_{measured}$ is the average value of measured data; $\overline{Z}_{modeled}$ is the average value of modeled results.

Meanwhile, the error analysis suggested by Ji (2008) was applied. Statistical variables such as Mean Error (ME), Root-Mean-Square Error (RMSE), and Relative Root-mean-square Error (RRE) were considered:

Table 2 Error analysis for measured and modeled water levels/flow rates

No.	Station	ME (m)	RMSE	RRE (%)
1	Bengbu Sluice	0.002	0.191	1.93
2	Wujiadu	0.038	0.213	2.24
3	Linhuaiguan	0.046	0.225	2.60
4	Wuhe	0.002	0.164	2.38
5	Fushan	-0.004	0.152	2.49
6	Xiaoliuxiang	-0.012	0.148	2.52
7	Xuyi	0.010	0.093	2.58
8	Laozishan	0.032	0.068	2.74
9	Jiangba	0.012	0.065	3.09
10	Gaoliangjian	-0.008	0.066	2.98
11	Shangzui	0.028	0.066	2.98
12	Linhuaitou	-0.018	0.071	3.12
13	Sanhe Sluice	0.029	0.067	3.48
14	Gaoliangjian Sluice	-0.004	0.067	3.04
15	Erhe Sluice	0.007	0.144	5.79
*6	Xiaoliuxiang	-37.638	198.897	2.59
*13	Sanhe Sluice	219.123	569.665	6.70

* Note, *stands for the station of discharge, and the unit is m³/s for ME and RMSE

$$ME = \frac{1}{N} \sum_{n=1}^{N} \left(Z_{modeled}^{n} - Z_{measured}^{n} \right) \tag{8}$$

$$RMSE = \sqrt{\frac{1}{N} \sum_{n=1}^{N} \left(Z_{modeled}^{n} - Z_{measured}^{n} \right)^2} \tag{9}$$

$$RRE = \frac{RMSE}{Z_{measured,max} - Z_{measured,min}} \tag{10}$$

where $Z_{measured,max}$ is the maximum value of measured data; $Z_{measured,min}$ is the minimum value of measured data.

The correlation indexes r and NSE were above 0.98 and 0.95, respectively, showing a consistent agreement between field measurements and numerical results (Figs. 7 and 8). The peak water levels of the two floods along the Huai River were both perfectly simulated, which is a pre-requisite to model the flooding process. The results of error analysis are listed in Table 2. RMSEs in water level were in the order of ~0.1–0.2 m and ~0.065 m for the riverine and lacustrine reaches, respectively. The RREs in water level were all within 3.5%, except for
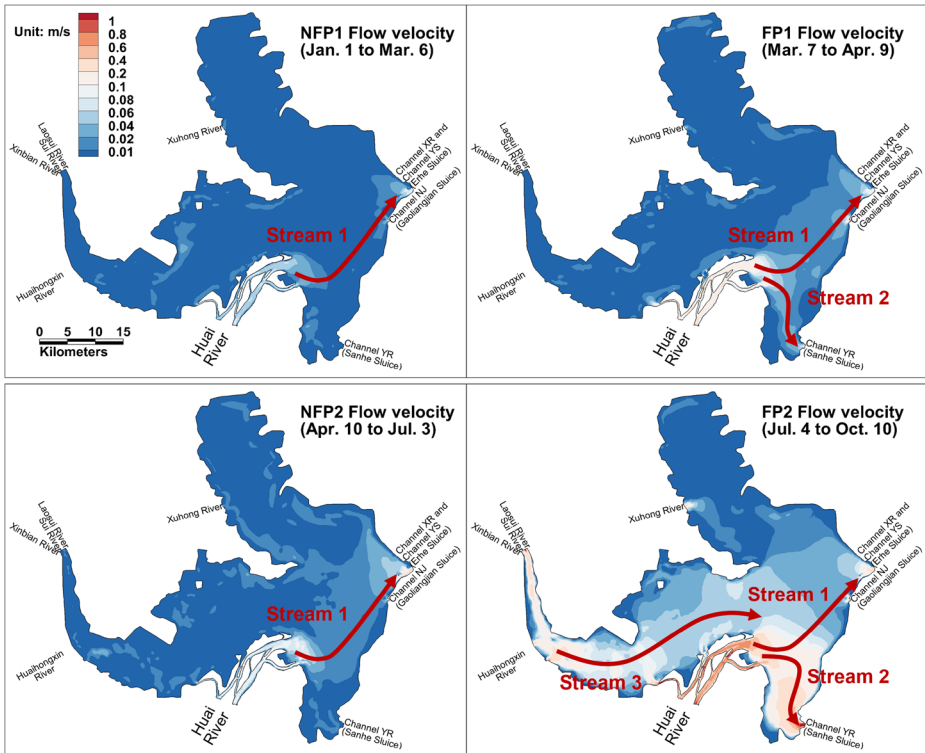

Fig. 10 Contour maps of seasonal-averaged flow velocity of Lake Hongze (Note, the velocity here is depth-averaged). The flow paths of three mainstreams are highlighted
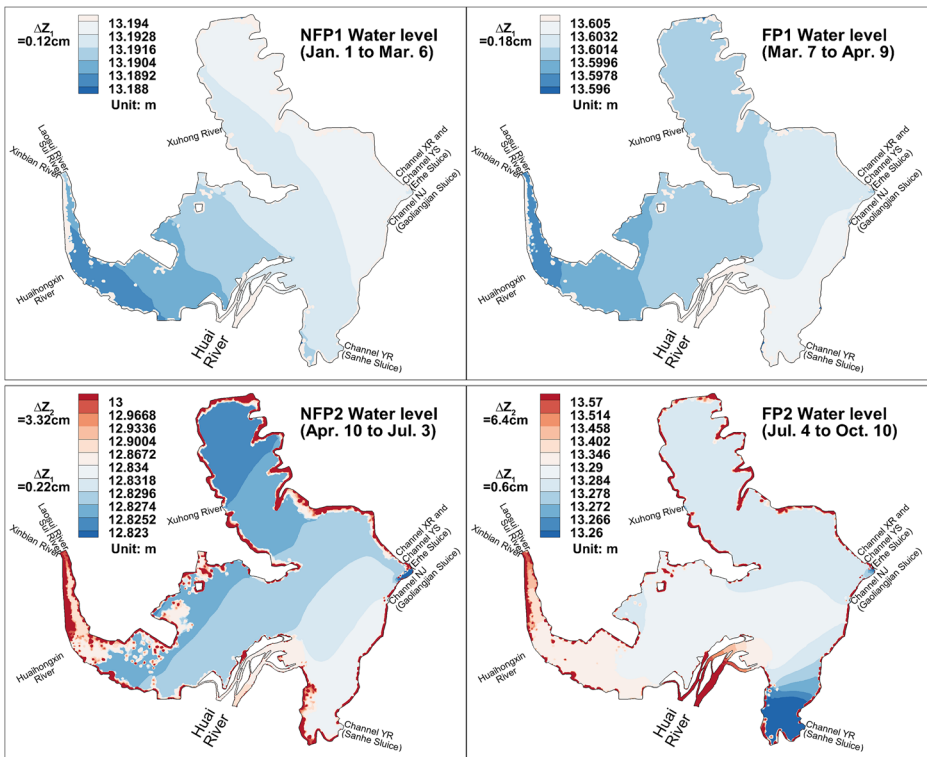
Fig. 11 Contour maps of seasonal-averaged water level of Lake Hongze (Note, ΔZ_1 is difference of water level contours in the main region, while in NFP2 and FP2, the level in Lihewa is much higher than other parts, hence which can be better shown by additional contours with a water level difference of ΔZ_2)

the station at the Erhe Sluice. A larger discrepancy at this location during the summer flood could be due to an insufficient grid resolution to model the narrow water diversion mechanism into the Erhe Sluice by a dike. However, this local difference had probably negligible effects on the large-scale hydrodynamics of the lake. RMSEs in flow rate were about 385 m^3/s for two key stations, and RREs in flow rate were about 4.65%. All in all, the performance of the model is satisfactory when applied to both riverine and lacustrine reaches.

4 Hydrodynamics of the River-lake System

The Huai River accounts for 86.48% of annual inflow into Lake Hongze in terms of volume, while Channel YR and Channel XR together with Channel YS convey 60.09% and 28.09% of annual outflow of the lake, respectively (Yu et al. 2017). Hence, the hydrodynamics of Lake Hongze is controlled mainly by the inflow from the Huai River and the outflows through the Sanhe Sluice and the Erhe Sluice. In the transition reach between the Huai River and Lake Hongze, the anabranching planform is remarkable, where the flow diversion in this reach is influenced by the downstream lake level and the upstream inflow. The seasonal variations of lake currents and the flow diversions in the anabranching reach are analyzed in details as follows.

4.1 Seasonal Variations of Lake Currents

The hydrodynamics of Lake Hongze have obvious characteristics of seasonal variations which are in consonance with the temporal distribution of the upstream inflows. The iso-vel maps of seasonal-averaged flow velocity, including the main flow patterns, and water level of Lake Hongze are presented in Figs. 10 and 11, respectively.

During the non-flood periods, i.e. NFP1, NFP2 and NFP3, the main flow pattern in the lake (Stream 1) was from the Huai River to the Erhe Sluice and the Gaoliangjian Sluice. In NFP1, the lake was fed by the Huai River, while other tributaries were providing water supply for local domestic, industrial and agricultural demands. Water level in the lake Z_{LH} was about 13.19 m (corresponds to a storage volume V_{LH} of 3.77 billion m^3), which decreases from northeast to southwest. The flow entering the lake rapidly decelerated and after 3.5 km it was in the order of about 0.01 m/s. Moreover, Stream 1 was deflected by the south-tilting basin topography flowing southeast first and then turning northeast.

In FP1, the composition of inflows was similar to that in NFP1. The peak discharge of the Huai River was 1950 m^3/s, equivalent to a once-in-a-year flood. Besides the perennial Stream 1, a second flow pattern (Stream 2) was created by opening of the Sanhe Sluice. The velocity of Stream 2 was 0.02–0.04 m/s, and its width was much narrower than that of Stream 1. The water level decreases from South Lake Hongze to Lihewa (west part), at about 13.6 m (corresponding V_{LH} = 4.39 billion m^3). The hydraulic gradient was around one and a half times larger than that in NFP1.

During NFP2, Z_{LH} = 12.83 m, which was lower than the other two water levels of the non-flood periods. The water level corresponding to NFP2 was maintained low by discharging over 1 billion m^3 of water from the lake following the flood of FP1. This was aimed to keep
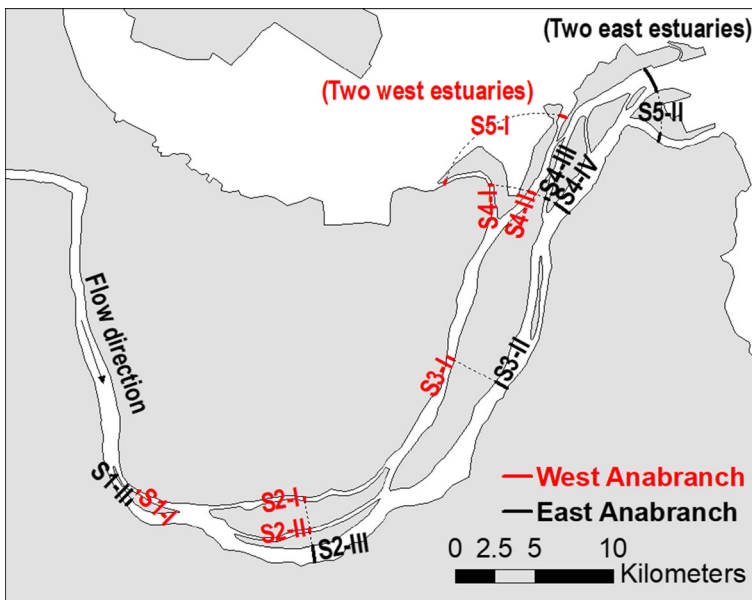

Fig. 12 Positions of cross-sections in the anabranching reach of the Huai River (Note, the West Anabranch includes the cross-sections of S1-I, S2-I, S2-II, S3-I, S4-I, S4-II, and the west two estuaries S5-I; the East Anabranch includes the cross-sections of S1-II, S2-III, S3-II, S4-III, S4-IV, and the east two estuaries S5-II)

provision to accommodate the flow of the oncoming flood, FP2. As precipitation increased over the Huai River Basin, all the feeding tributaries were discharging into the lake. Stream 1 had a velocity, 0.01–0.02 m/s, larger than that in NFP1 due to both the shallower water depth and larger discharge. The water level in Lihewa was slightly higher than that in the central region of the lake, by about 0.1 m.

In FP2, floods occurred in the Huai River and other feeding tributaries. A peak total inflow of 10,010 m³/s occurred on July 20. The discharge of the Huai River Q_{HR} was 7770 m³/s, equivalent to a once-in-twenty-year flood. Stream 2 had a high velocity zone of 0.2–0.4 m/s, indicating a scour-prone region. It should be noted that the median diameter d_{50} of the lacustrine suspended sediment is 14.74 μm according to the field measurement by Lei et al. (2019). Using an empirical formula for sediment incipient motion, after Einstein (Eq. 11;
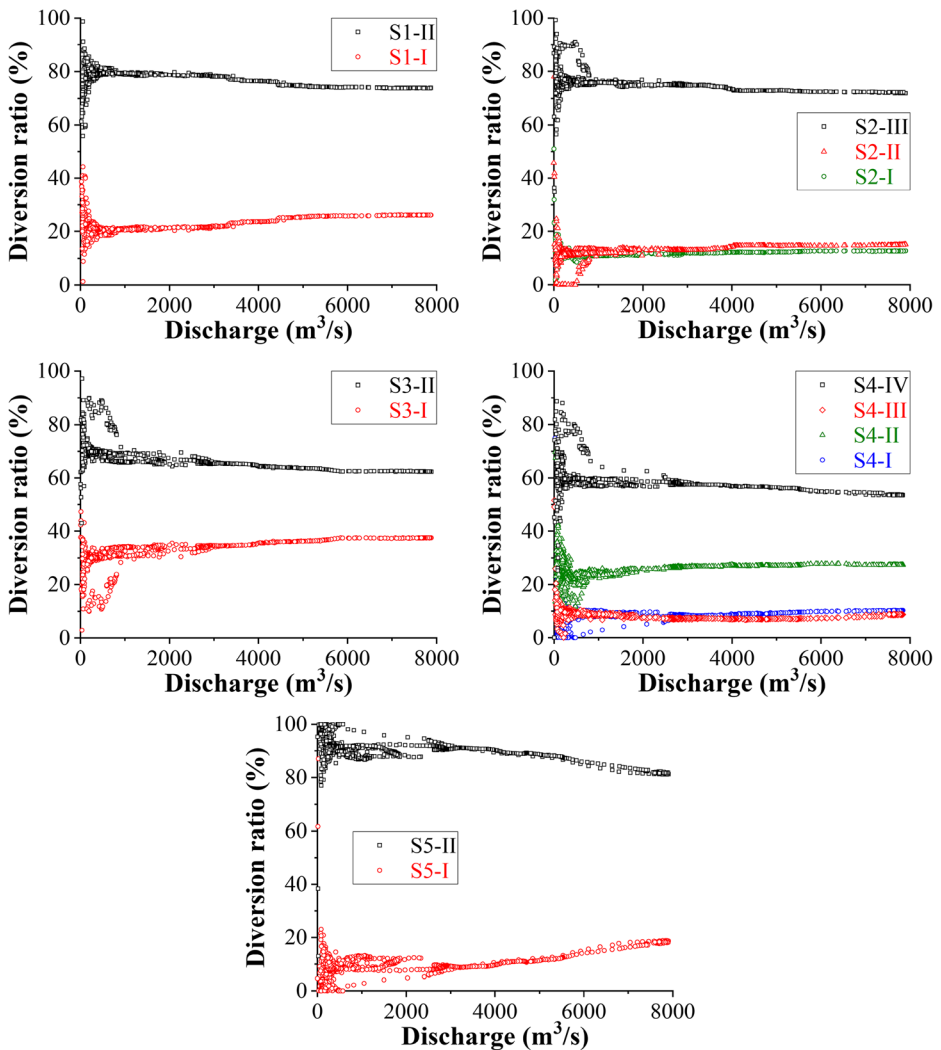

Fig. 13 Relationships between diversion ratio and discharge in five locations in the anabranching reach of the Huai River

Chien and Wan 1999), the critical incipient velocity v_c was estimated as 0.238 m/s. Moreover, Stream 3 flowing from Lihewa to join Streams 1 and 2, appeared during the big flood. The velocity of Stream 3 also exceeded v_c. The water level in the central region of the lake was about 13.29 m (corresponding V_{LH} = 3.91 billion m³). The water level in Lihewa was 0.15 m higher. Finally, in NFP3, no significant difference in the spatial distributions of velocity and water level from NFP1 was predicted. Therefore, separate results for NFP3 are not included here.

$$v_c = 5.75 \sqrt{\Theta_c} \sqrt{\frac{\gamma_s - \gamma_w}{\gamma_w} g d_{50}} \log\left(12.27 \frac{\chi h}{d_{50}}\right) \tag{11}$$

where Θ_c is critical shields number; γ_s and γ_w are bulk density of sediment and water, respectively; χ is parameter reflecting transition from smooth to rough boundary; h is water depth.

4.2 Flow Diversion in the Anabranching Reach of the Huai River

The transition reach of the Huai River - Lake Hongze system from Fushan to Laozishan, a sharp meander bend, is 84 km long and on average 730 m wide. The river planform is shaped with a right-angled bend (Fig. 3) followed by anabranching patterns (Fig. 12), that is the river shows a multi-channel structure. This structure is believed to be very common in large rivers (Latrubesse 2008).

In the anabranching rivers, the diversion discharge ratio, defined as the ratio of discharge of each branch to the total upstream discharge, is a major parameter which affects the hydrodynamics and sediment transport (Du et al. 2016). In 2010, a normal flow year, annual-averaged total suspended sediments (*TSS*) concentration decreased from 73.5 mg/L at Wujiadu to 65.4 mg/L at Xiaoliuxiang and 18.4 mg/L at Laozishan as deposition occurred mainly downstream of the right-angled bend (Cao et al. 2017).

The anabranching reach can be broadly divided into two main branches, i.e. the West Anabranch and the East Anabranch. Five locations, having thirteen cross-sections, were considered in this reach (Fig. 12). The relationship between the diversion ratio and the discharge in these cross-sections is illustrated in Fig. 13. The lake level and the ensuing flow diversion varies accordingly. The results show that the diversion ratios are not single-valued for the low discharges (basically lower than 2000 m³/s), because of the rather dramatically-changed water depth and river width caused by the variation of the lake level. As the discharge increases, the diversion ratio of the West Anabranch increases at all the locations considered.

Table 3 Flow diversion ratios (Unit: %) for a once-in-twenty-year flood in the anabranching reach of the Huai River

Anabranch no.	Location no.				
	1	2	3	4	5
I	26.2	12.7	37.5	10.2	18.0
II	**73.8**	15.1	**62.5**	27.5	**82.0**
III	/	**72.2**	/	**8.6**	/
IV	/	/	/	**53.7**	/

*Diversion ratios are bolded for the East Anabranch

The rate of increase is maximum at S5 as if the upstream discharge increases from 4000 to 8000 m³/s. The diversion ratio of the West Anabranch increases from 10% to nearly 20%.

The floodwater diversion ratio for a once-in-twenty-year flood ($Q_{HR} \approx 8000$ m³/s) at the considered stations is listed in Table 3. The results show that the East Anabranch acts as the main branch accounting for more than 82% of the inflow of the Huai River. Hence, in the subsequent presentation, the water surface profile of the East Anabranch will be considered to represent that of the entire anabranching reach.

5 Discussion on Mechanism of the Prolonged Flooding

The uppermost mitigation solution to the river flooding is to lower the lake level (Case 1), thereby to increase the hydraulic gradient. Numerical simulations were carried out with different water levels in the lake. For a small flood ($Q_{HR} = 4710$ m³/s), four levels, 12.4 m, 12.9 m, 13.4 m, and 13.9 m, were considered. It should be noted that the warning line of the lake level for flood control is 13.5 m, and the highest water level at the Sanhe Sluice was 13.88 m on May 4, 2008. The results are shown in Fig. 14. The backwater effect of Lake Hongze can be observed mainly downstream of Xuyi, which is located approximately 30 km upstream of the lake. Near the right-angled bend (Fig. 3), the backwater effect vanishes. The backwater effect is smaller even for larger discharge in the Huai River. Therefore, the option to lower the water level in the lake has only a modest impact on prolonged flooding. Consequently, the limiting criterion for the lake level during/before the flood season can be set a bit higher. For example, discarding the practice of pre-release operation during NFP2, the available water resources can be increased by 1 billion m³ (Sect. 3.1), which results in 30% increment. The impact of raising the lake level on ecological system was evaluated by Lin et al. (2017). The abundance and distribution of submerged macrophytes, further the dominance of different fish assemblages would be severely changed. The trade-off between water resources increment and water environment conservation should be further investigated. The surface water resources and the groundwater resources in the middle Huai River Basin are 26.9 and 16.7 billion m³, respectively, on a multi-year average (The Huaihe River Commission of the Ministry of Water Resources 2019). Few references are available about the water exchange between the river and the groundwater in this region. This could be the objective of future studies.
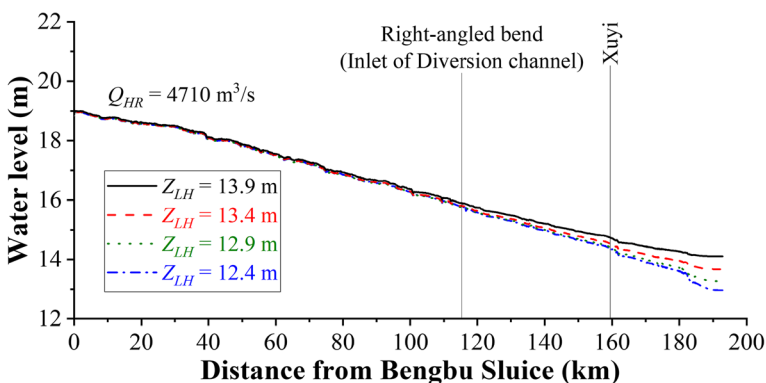

Fig. 14 Backwater effect of different lake levels

Another possible explanation is the effects of the negative bed slope at the mouth of the Huai River. Two dredging plans (Case 2) were considered in the reach from Fushan to Laozishan. The first plan (Case 2A) is aimed at eliminating the negative bed slope and provide the same positive slope existing in the upper reach, that is 0.06‰. The dredging depth in this case is proportional to the distance from the origin of the negative bed slope, as Fig. 4 shows, and the current cross-section would be maintained. The elevation of the lake basin also should be lowered with an identical dredging depth of 8.225 m, to match with the dredging depth at the end of the modified-bed-slope reach. The second dredging plan (Case 2B) is to lower the lake basin to the elevation of the floor slab at the Sanhe Sluice, which is 7.5 m. As the current elevation of the lake basin is around 10.5 m, the dredging depth there would be 3.0 m and the river bed slope will raise from -1.17‰ to -0.72‰.

The two dredging options are compared, and the simulated surface water profiles for $Q_{HR} = 7770$ m³/s are presented in Fig. 15. With the elimination of the negative bed slope in the transition reach, the effect of the lake level extends upstream. The plunge point, where the river level is equal to the lake level, is located for Cases 2A and 2B at 20 and 65 km downstream from the right-angled bend, respectively. Therefore, the hydraulic gradient will increase significantly and the water level along the Huai River would be lowered. A similar phenomenon can be observed in the river-reservoir system, for instance, the Weihe River (the largest tributary of the Yellow River) and the Sanmenxia Reservoir (first-built reservoir in the Yellow River for sediment regulation). However, with the impoundment of the reservoir, serious sedimentation occurred in backwater region within one year, changing the bed elevation at the confluence of the Weihe River and reservoir (Wang et al. 2007) and creating continuous deposition in the Weihe River and, thus, serious flooding.

The aggradation is a feedback process in the backwater region. Hence, the dredging plan cannot change the long-term evolution, especially in the plain area. Moreover, the dredging plan extends over 84-km river reach and the entire lake area. This will be harmful to the local aquatic ecosystem. A feasible management plan (Case 3) was considered, that is to create a diversion channel near the right-angled bend (Fig. 3). Information about the diversion channel are presented in Fig. 5. The channel can not only broaden the flow passage, but also create an alternative option to avoid the additional backwater. The channel can divert almost half of the
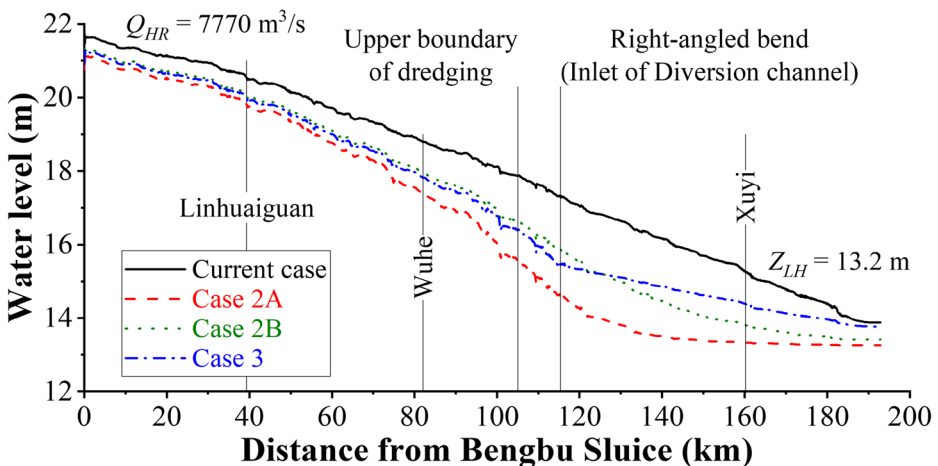

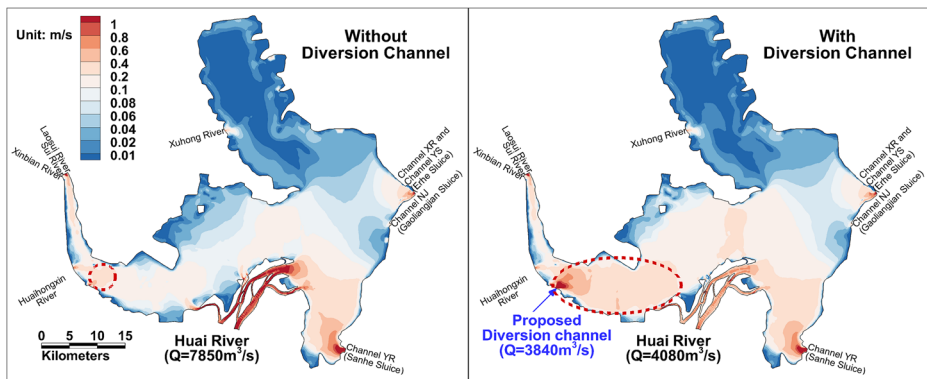**Fig. 15** Simulated surface water profiles for different management plans

Fig. 16 Spatial distributions of the depth-averaged velocity in the lake area without or with the proposed diversion channel. The scour-prone regions are marked by red dashed circles

peak flood (Fig. 16). The simulated water surface profiles for Q_{HR} = 7770 m³/s are plotted in Fig. 15. The largest drop in water level takes place at the inlet of the diversion channel, which is 1.9 m. The drops are 0.4 and 0.1 m at river begin and end, respectively. The diversion channel can alter the local planform and be helpful to drain the floodwater fast. Furthermore, the diversion channel, by lowering the lake level will also directly increase the head difference, which, in turn, is beneficial to a further decrease of the water level in the Huai River. It is noticeable that the major difference between Cases 2B and 3 occurs downstream of the inlet to the diversion channel. Therefore, for relieving the pressure of fast flood drainage in the upper reach, the diversion channel has a performance comparable with that of Case 2B.

River channels are naturally straightened by meander bends cutting, which shortens the flow path and increases the hydraulic gradient (Hudson and Kesel 2000). Meander bend cutoffs usually occur in the reach with a large sinuosity. The flow continuously erodes the outer bend and finally connects with the downstream reach in a shorter way. In this process, the old channel is subjected to continuous deposition. In the Huai River - Lake Hongze system, the influence of the lake on the river is extending up to the right-angled bend. The proposed diversion channel is intended to reproduce the natural process of meander bend cutoff, which has been largely limited by intensively built and reinforced embankments. This kind of measure is beneficial to flood mitigation strategies for similar river-lake systems.

Figure 16 shows the distribution of the depth-averaged velocity in the lake for Case 3, where the scour-prone region would be two times larger than that without the diversion channel. At the outlet of the diversion channel, *TSS* concentration is currently lower than the average value in the lake (Cao et al. 2017). In Case 3, it is expected that scouring in that region will increase *TSS* concentration and water turbidity negatively affecting algae and aquatic plants growth (Ren et al. 2014).

6 Conclusions

In this paper, lake hydrodynamics was studied during non-flood and flood periods of a year with a 3-D model, and flow diversions in the anabranching reach were correlated with upstream discharge. Further, numerical simulations were carried out to investigate the cause of prolonged flooding by the Huai River. Finally, different, alternative measures to address this problem were comparatively discussed. The main findings from this numerical study are:

(1) Four different phases of flow were identified and the hydrodynamic aspects in the lake, corresponding to each, were described in detail. Three main flow patterns were observed.

(2) The East Anabranch of Huai River is the predominant branch which accounts for over 82% of the inflow from the river to the lake.

(3) The water level of Lake Hongze can affect the flow regime in the Huai River, downstream of the right-angled bend. However, its influence seems to be limited in tackling the prolonged flooding problem. The common practice of pre-release operation of the stored water seems useless, while avoiding this operation can increase the available water resources by about 1 billion m^3.

(4) The sediment bar in the mouth of the Huai River was related to the formation of Lake Hongze, which caused retrogressive sedimentation up to near the right-angled bend. The resulting negative bed slope reduces the hydraulic gradient leading to additional backwater. Moreover, near the right-angled bend, the channel cross-section is narrowed and more energy is dissipated. In summary, the floodwater cannot be drained fast and the effect of lake level lowering may be limited.

(5) The proposed diversion channel, to directly connect the lake and the river near the right-angled bend, would lead to a broad flow passage, a short river flow path and further a large hydraulic gradient. This solution provides a performance comparable to the dredging plan but with a lower environmental impact and a longer-term effect.

The main conclusive remarks on river-lake hydrodynamic interactions can be summarized as: (1) lowering the lake level to reduce its effects on flooding in the river would have limited effect, that would be rapidly impaired by the sharp meander bend connecting the river and the lake, (2) the artificial cutoff of this intensively-embanked bend has great potential in reducing the river stage and flood damages, as the construction of a diversion channel would shorten the flow path and increase the hydraulic gradient.

To further study and manage the river-lake interactions, the following issues should be considered:

• The long-term evolution of river channel and lake basin, which is required for sustainable management;

• The spatiotemporal distribution of water quality index and its influence on the algal dynamics;

• The ecological effects associated with the change of the lake level on fisheries as well as the benefits related to the large volume of water available in the lake.

Compliance with Ethical Standards

Conflict of Interest None.

References

Bai X, Wang J, Schwab DJ, Yang Y, Luo L, Leshkevich GA, Liu S (2013) Modeling 1993–2008 climatology of seasonal general circulation and thermal structure in the Great Lakes using FVCOM. Ocean Model 65:40–63

Ben P (2010) The research and application of the hydrodynamic mathematical model on the middle part of Huai River between Bengbu Gate to Laozishan. Hefei University of Technology (in Chinese)

Ben-Dan TB, Shteinman B, Kamenir Y, Itzhak O, Hochman A (2001) Hydrodynamical effects on spatial distribution of enteric bacteria in the Jordan River - Lake Kinneret contact zone. Water Res 35:311–314

Cao Z, Duan H, Feng L, Ma R, Xue K (2017) Climate- and human-induced changes in suspended particulate matter over Lake Hongze on short and long timescales. Remote Sens Environ 192:98–113

Chen CS, Liu HD, Beardsley RC (2003) An unstructured grid, finite-volume, three-dimensional, primitive equations ocean model: Application to coastal ocean and estuaries. J Atmos Ocean Technol 20:159–186

Chen C, Beardsley RC, Cowles G (2006) An unstructured grid, finite-volume coastal ocean model (FVCOM) system. Oceanography 19:78–89

Chien N, Wan Z (1999) Mechanics of sediment transport. American Society of Civil Engineers, Reston

Dai M, Wang J, Zhang M, Chen X (2017) Impact of the Three Gorges Project operation on the water exchange between Dongting Lake and the Yangtze River. Int J Sedim Res 32:506–514

Du Q, Tang H, Yuan S, Xiao Y (2016) Predicting flow rate and sediment in bifurcated river branches. Proc Inst Civ Eng Water Manag 169:156–167

Galperin B, Kantha L, Hassid S, Rosati A (1988) A quasi-equilibrium turbulent energy model for geophysical flows. J Atmos Sci 45:55–62

Gualtieri C, Ianniruberto M, Filizola N (2019) On the mixing of rivers with a difference in density: The case of the Negro/Solimões confluence, Brazil. J Hydrol 578:124029

Han R, Suryadi FX (2004) Flood control and land use management in Mengwa retention area, Huai River Basin. Irrig Sci 53(4):385–395

He C, Rao YR, Skafel MG, Howell T (2006) Numerical modelling of the Grand River plume in Lake Erie during unstratified period. Water Qual Res J Can 41:16–23

Huang W, Li C (2017) Cold front driven flows through multiple inlets of Lake Pontchartrain Estuary. Journal of Geophysical Research: Oceans 122(11):8627–8645

Hudson PF, Kesel RH (2000) Channel migration and meander-bend curvature in the lower Mississippi River prior to major human modification. Geology 28(6):531–534

Hudson PF, Middelkoop H, Stouthamer E (2008) Flood management along the Lower Mississippi and Rhine Rivers (The Netherlands) and the continuum of geomorphic adjustment. Geomorphology 101(1–2):209–236

Ianniruberto M, Trevethan M, Pinheiro A, Andrade JF, Dantas E, Filizola N, Santos A, Gualtieri C (2018) A field study of the confluence between Negro and Solimoes Rivers. Part 2: Bed morphology and stratigraphy. CR Geosci 350:43–54

Ji Z-G (2008) Hydrodynamics and water quality: Modeling rivers, lakes, and estuaries. Wiley, Hoboken

Latrubesse EM (2008) Patterns of anabranching channels: The ultimate end-member adjustment of mega rivers. Geomorphology 101:130–145

Lei S, Wu D, Li Y, Wang Q, Huang C, Liu G, Zheng Z, Du C, Mu M, Xu J, Lv H (2019) Remote sensing monitoring of the suspended particle size in Hongze Lake based on GF-1 data. Int J Remote Sens 40:3179–3203

Lin CA, Wen L, Lu G, Wu Z, Zhang J, Yang Y, Zhu Y, Tong L (2010) Real-time forecast of the 2005 and 2007 summer severe floods in the Huaihe River Basin of China. J Hydrol 381(1–2):33–41

Lin ML, Lek S, Ren P, Li SH, Li W, Du X, Guo CB, Gozlan RE, Li ZJ (2017) Predicting impacts of south-to-north water transfer project on fish assemblages in Hongze Lake, China. J Appl Ichthyol 33:395–402

Liu K, Yao C, Chen J, Li Z, Li Q, Sun L (2017) Comparison of three updating models for real time forecasting: a case study of flood forecasting at the middle reaches of the Huai River in East China. Stoch Env Res Risk Assess 31:1471–1484

Mellor GL, Yamada T (1982) Development of a turbulence closure model for geophysical fluid problems. Rev Geophys 20:851–875

Ministry of Water Resources of the People's Republic of China (2019) Bulletin of flood and drought disasters in China. China Water & Power Press, Beijing (in Chinese)

Nash JE, Sutcliffe JV (1970) River flow forecasting through conceptual models part I—A discussion of principles. J Hydrol 10(3):282–290

Nekouee N, Hamidi SA, Roberts PJW, Schwab DJ (2015) Assessment of a 3D Hydrostatic Model (POM) in the Near Field of a Buoyant River Plume in Lake Michigan. Water Air Soil Pollut 226

Paturi S, Boegman L, Rao YR (2012) Hydrodynamics of eastern Lake Ontario and the upper St. Lawrence River. J Great Lakes Res 38:194–204

Qian M, Wang K (2017) Flood management in China: The Huaihe River Basin as a case study. In: Hromadka T (ed) Flood Risk Management. InTech, London, pp 129–152

Rao YR, Zhao J (2010) Numerical simulation of the influence of a Red River flood on circulation and contaminant dispersion in Lake Winnipeg. Nat Hazards 55:51–62

Ren Y, Pei H, Hu W, Tian C, Hao D, Wei J, Feng Y (2014) Spatiotemporal distribution pattern of cyanobacteria community and its relationship with the environmental factors in Hongze Lake, China. Environ Monit Assess 186:6919–6933

Shore JA (2009) Modelling the circulation and exchange of Kingston Basin and Lake Ontario with FVCOM. Ocean Model 30:106–114

Smagorinsky J (1963) General circulation experiments with the primitive equations: I. The basic experiment. Mon Weather Rev 91:99–164

Sokolov AA, Chapman TG (1974) Methods for water balance computations; an international guide for research and practice-A contribution to the International Hydrological Decade. France) UNESCO, Paris

Sorensen J, Sydor M, Huls H, Costello M (2004) Analyses of Lake Superior seiche activity for estimating effects on pollution transport in the St. Louis River estuary under extreme conditions. J Great Lakes Res 30:293–300

The Huaihe River Commission of the Ministry of Water Resources (2019) The huai river water resources bulletin (in Chinese)

Wan X, Hua L, Yang S, Gupta HV, Zhong P (2018) Evaluating the impacts of a large-scale multi-reservoir system on flooding: Case of the Huai River in China. Water Resour Manag 32:1013–1033

Wang Q, Chen J (1999) Formation and evolution of Hongze Lake and the Huaihe River mouth along the lake. J Lake Sci 11:244–249 (in Chinese)

Wang Z-Y, Wu B, Wang G (2007) Fluvial processes and morphological response in the Yellow and Weihe Rivers to closure and operation of Sanmenxia Dam. Geomorphology 91:65–79

Wang P, Lai G, Li L (2015) Predicting the hydrological impacts of the Poyang Lake project using an EFDC model. J Hydrol Eng 20

Wu J, Zeng H, Yu H, Ma L, Xu L, Qin B (2012) Water and sediment quality in lakes along the middle and lower reaches of the Yangtze River, China. Water Resour Manag 26:3601–3618

Yu B-y, Wu P, Sui J-y, Yang X-j, Ni J (2014) Fluvial geomorphology of the Middle Reach of the Huai River. Int J Sedim Res 29:24–33

Yu B-y, Cai J-p, Huang L-m, et al (2017) Hydrodynamic numerical model of the middle reach of the Huai River and its application. China Water & Power Press (in Chinese)

Zhang X, Song Y (2014) Optimization of wetland restoration siting and zoning in flood retention areas of river basins in China: A case study in Mengwa, Huaihe River Basin. J Hydrol 519:80–93

Zhang Y, Xia J, Liang T, Shao Q (2010) Impact of water projects on river flow regimes and water quality in Huai River basin. Water Resour Manag 24:889–908

Zhang J, Feng L, Chen L, Wang D, Dai M, Xu W, Yan T (2018) Water compensation and its implication of the Three Gorges Reservoir for the River-Lake System in the Middle Yangtze River, China. Water 10

Zhao Y, Gong Z, Wang W, Luo K (2014) The comprehensive risk evaluation on rainstorm and flood disaster losses in China mainland from 2004 to 2009: based on the triangular gray correlation theory. Nat Hazards 71:1001–1016

Zheng W, Liu C, Xin Z, Wang Z (2008) Flood and waterlogging monitoring over Huaihe River Basin by AMSR-E data analysis. Chin Geogra Sci 18(3):262–267

Publisher's Note Springer Nature remains neutral with regard to jurisdictional claims in published maps and institutional affiliations.